



# Novel Biodegradable Thermoplastic Elastomer Based on Poly(butylene succinate) and Epoxidized Natural Rubber Simple Blends

Parisa Faibunchan<sup>1</sup> · Yeampon Nakaramontri<sup>1</sup> · Wannarat Chueangchayaphan<sup>1</sup> · Skulrat Pichaiyut<sup>1</sup> · Claudia Kummerlöwe<sup>2</sup> · Norbert Vennemann<sup>2</sup> · Charoen Nakason<sup>1</sup>

Published online: 11 January 2018  
© Springer Science+Business Media, LLC, part of Springer Nature 2018

## Abstract

Novel biodegradable thermoplastic elastomer based on epoxidized natural rubber (ENR) and poly(butylene succinate) (PBS) blend was prepared by a simple blend technique. Influence of blend ratios of ENR and PBS on morphological, mechanical, thermal and biodegradable properties were investigated. In addition, chemical interaction between ENR and PBS molecules was evaluated by means of the rheological properties and infrared spectroscopy. Furthermore, the phase inversion behavior of ENR/PBS blend was predicted by different empirical and semi-empirical models including Utracki, Paul and Barlow, Steinmann and Gergen models. It was found that the co-continuous phase morphology was observed in the blend with ENR/PBS about 58/42 wt% which is in good agreement with the model of Steinmann. This correlates well to morphological and mechanical properties together with degree of crystallinity of PBS in the blends. In addition, the biodegradability was characterized by soil burial test after 1, 3 and 9 months and found that the biodegradable ENR/PBS blends with optimum mechanical and biodegradability were successfully prepared.

**Keywords** Biodegradability · Bio-based thermoplastic · Poly(butylene succinate) · Epoxidized natural rubber

## Introduction

Polymer blends are typically prepared by mixing at least two different types of polymeric materials to create new types of materials with more desired properties. Thermoplastic elastomer (TPE) is one interesting type of polymer blends which combine performance and properties of conventional vulcanized rubbers with processability of thermoplastics. The TPE based on blending of elastomers and thermoplastics can be categorized into two main groups: simple blends (SBs) and dynamic vulcanizates (DVs) or thermoplastic vulcanizates (TPVs). Typically, the SBs are prepared by blending the elastomer and thermoplastic pairs without addition of any curatives during blending operation with the final blend

morphology as the co-continuous or dual phase structures. On the other hand, the TPVs are prepared by incorporating of curatives during mixing operation. The final morphology or phase structure of TPVs is dispersion of micron sized vulcanized rubber domains in the thermoplastic matrix.

Natural rubber (NR) is exploited as one of elastomeric component in preparation of TPE material which is typically called as thermoplastic natural rubber (TPNR) [1]. Typically, NR is an attractive bio-based elastomer due to its excellent properties including high elasticity, mechanical strength, fatigue resistance and tear strength together with environmental friendliness. Apart from the normal NR form, the chemically modified NRs, such as epoxidized natural rubber (ENR), have also been used to prepare the TPNR owing to its unique properties including high polarity and air impermeability. There are many kinds of thermoplastics that have been used to prepare TPNR based on blending with ENR, such as polyolefin [2, 3], poly(vinyl chloride) [4, 5], polyamide (PA) [6, 7], and polyester [8, 9].

Biodegradable materials has been increasingly interested currently due to growing concern of the environmental awareness. The replacement of the conventional non-biodegradable materials has been common practices

✉ Charoen Nakason  
charoen.na@psu.ac.th

<sup>1</sup> Department of Rubber Technology, Faculty of Science and Industrial Technology, Prince of Songkla University, Surat Thani Campus, Surat Thani 84000, Thailand

<sup>2</sup> Faculty of Engineering and Computer Science, University of Applied Sciences Osnabrück, Albrechtstrasse 30, 49076 Osnabrück, Germany

in many applications [10]. Poly(butylene succinate) (PBS) is one of biodegradable aliphatic polyesters that has been used for such purpose. Typically, PBS exhibits good mechanical properties and several useful properties for industries including good melt processibility, high chemical resistance, thermal properties and biodegradability [11, 12]. Several attempts have been made on blending of PBS with other polymers including polylactic acid (PLA) [12–14], poly-L-lactic acid (PLLA) [15], thermoplastic starch (TPS) [16], nitrile rubber (NBR) [17], and thermoplastic polyurethane (TPU) [18]. On the other hand, NR has also been used to prepare biodegradable polymers by blending with various polymers such as PLA [19], and TPS [20]. It is noted that NR has been known as the renewable resourced material, but it is not readily biodegradable especially in the form of vulcanizates. To accelerate biodegradation of NR materials, blending of NR with other biodegradable thermoplastics such as PBS might be one of a possible route to obtain a biodegradable elastomer based on NR. The blend product may be promising to be used as bio-based TPE materials.

In the present work, SBs of ENR with 50 mol% epoxides (i.e., ENR-50) and PBS (i.e., ENR/PBS blends) were prepared with various ENR/PBS proportions in the ranges of 80/20, 70/30, 60/40, 50/50, 40/60, 30/70, and 20/80 wt%. The main aim was to prepare the TPNR with co-continuous phase morphology and acceptable mechanical and other related properties for industrial applications. Furthermore, four semi-empirical models include Utracki [21], Paul and Barlow [22], Steinmann [23] and Gergen [24] models were used to predict the phase inversion behavior of the ENR/PBS blends. The indication of phase inversion at different biodegradable states was also identified by morphological characterization. In addition, rheological, mechanical, thermal and biodegradable properties of the blends with different blend ratios were also examined.

## Experimental

### Materials

ENR with 50 mol% epoxides (i.e., ENR-50) was used as the rubber component in ENR/PBS blends. It was manufactured by Muang Mai Guthrie Co. Ltd. (Surat Thani, Thailand). PBS, Bionolle™ 1001 MD, was used as thermoplastic blend component. It was manufactured by Showa Denko Co. Ltd. (Tokyo, Japan). In addition, Wingstay-L was used as an antioxidant, manufactured by Eliokem Inc. (OH, USA). Some specific properties of the chemicals used in this work are summarized in Table 1.

**Table 1** Specific properties of the chemicals used in the ENR/PBS blends

Materials	Properties	
ENR-50	Epoxidation level (%)	50 ± 2
	Specific gravity	1.03
	Mooney viscosity ML (1 + 4) 100 °C	70–100
	Ash content (%)	0.50
PBS	Specific gravity	1.26
	Melting point (°C)	114
	Degree of crystallinity (%)	30–35
	Glass transition temperature (°C)	–32
Wingstay-L	Specific gravity	1.10
	Average molecular weight (g/mol)	650
	Melting point (°C)	115
	Ash content (%)	0.10

### Preparation of ENR/PBS Simple Blends

ENR and PBS were first dried in a hot air oven at 60 °C for 24 h to remove moisture before blending. Two mixing steps were exploited by first masticating of ENR in an internal mixer with a mixing chamber capacity of 500 cm<sup>3</sup> (Chareon tut Co. Ltd., Samut Sakorn, Thailand) for 1 min at a rotor speed of 60 rpm at 60 °C. Then, 1 phr of Wingstay-L antioxidant was added and continuously mixed for another 4 min before sheeting out on two-roll mills. The ENR/Wingstay-L mixture was then conditioned at room temperature for at least 24 h before blending with PBS. In the second step, PBS was initially incorporated into the mixing chamber with continuously rotated at a rotor speed of 60 rpm for 4 min at 120 °C. The ENR/Wingstay-L mixture was consequently incorporated and continued mixing for another 4 min to gain the total mixing time of 8 min. The ENR/PBS blends were eventually dumped from the mixing chamber and again sheeted out before conditioning at room temperature for at least 24 h. Finally, the blends were fabricated by compression molding at 150 °C to form a thin sheet with 1 mm thickness before testing and characterizing. It is noted that the ENR/PBS blends with various blend proportions of ENR/PBS = 80/20, 70/30, 60/40, 50/50, 40/60, 30/70, and 20/80 wt% were prepared and characterized.

### Dynamic Properties

Complex viscosity ( $\eta^*$ ) of pure parent polymer pairs (i.e., PBS and ENR) were determined using a rubber process analyzer, RPA 2000 (Alpha Technologies, Akron, USA). The frequency sweep test in the ranges of 2–30 rad/s was performed at 150 °C.

## Rheological Characterization

Rheological properties of pure parent polymer pairs were characterized using a high pressure capillary rheometer with a twin barrel system model Rheograph 25 (GÖTTFERT Werkstoff-Prüfmaschinen GmbH, Buchen, Germany). The shear rate ranges were set at 50–1250 s<sup>-1</sup>. Dimension of the capillary die used was 2 mm in diameter and 32 mm in length. In order to get a compact mass, the samples were first incorporated into the barrel of the rheometer and then preheated for 5 min under a pressure of approximately 3–5 MPa. The apparent shear viscosity,  $\eta_s$  (Pa s), the apparent shear rate  $\dot{\gamma}_{app}$  and shear stress  $\tau_w$  at the wall of the capillary were calculated by the following equations [25]:

$$\tau_w = \frac{R\Delta P}{2L} \quad (1)$$

$$\dot{\gamma}_{app} = \frac{4Q}{\pi R^3} \quad (2)$$

$$\eta_s = \frac{\tau_w}{\dot{\gamma}_{app}} \quad (3)$$

where  $\Delta P$  is the pressure drop along the die (Pa),  $Q$  is the volumetric flow rate (m<sup>3</sup>/s) and  $R$  is the capillary radius (m).

## Morphological Properties

Morphological properties were determined by scanning electron microscope (SEM) (FEI-Quanta 400, OR, USA) and digital light microscope (Shenzhen TongShunHui AV Technology Co., Ltd, Guangdong, China). The specimens were first cryogenic fractured after immersing in liquid nitrogen and then etched by extracting the ENR phase with toluene for 20 min. The extracted samples were eventually dried at room temperature for at least 48 h to remove the solvent. The samples were then gold sputter-coated before SEM characterization. It is noted that the morphological properties of blend samples after 9 months soil burial were also examined without surface treatment.

## Mechanical Properties

Mechanical properties in terms of 100% modulus, tensile strength, elongation at break and tension set of the pure PBS and ENR/PBS simple blends were characterized by a tensile testing machine model 10ST (Tinius Olsen, Salfords, England) according to ISO 37 and ISO 2285 (tension set), respectively. In addition, hardness of the blend samples was also measured by durometer Shore A model Instron Shore

S1 digital durometer (Instron, Norwood, USA) following ISO 868.

## Thermal Properties

Thermal properties of the pure parent polymer pairs and ENR/PBS simple blends were characterized by the differential scanning calorimeter model DSC823e (Mettler Toledo, Greifensee, Switzerland). The DSC test was performed using a heating rate of 10 K/min under nitrogen atmosphere. The first heating scan was performed in the temperature ranges of –60 to 200 °C to eliminate the thermal history of the materials. Then, the samples were cooled down from 200 to –60 °C, and heated again from –60 to 200 °C with the same cooling and heating rates of 10 K/min. The first cooling scan (1st) and second heating scan (2nd) were then recorded as the endothermic and exothermic thermograms. Thus, glass transition temperature ( $T_g$ ), crystalline melting temperature ( $T_m$ ) and crystallization temperature ( $T_c$ ) of the pure parent polymer pairs and ENR/PBS simple blends were identified based on the DSC thermograms. Also, the crystallization enthalpy ( $\Delta H_c$ ) and the heat of fusion ( $\Delta H_m$ ) were determined based on the area of crystallization and melting peaks, respectively.

## Soil Burial Test

The soil burial test was performed in order to examine the biodegradability of the pure polymers and ENR/PBS simple blends. The dumbbell shaped specimens were prepared and buried in soil with a depth of 0.07 m. The specimens were buried for different time periods of 1, 3 and 9 months before cleaning by clean water. The samples were then dried at 60 °C for 24 h. The weight loss of the samples was calculated following Eq. (4):

$$\text{Weight loss (\%)} = \frac{W_0 - W_t}{W_0} \times 100 \quad (4)$$

where  $W_0$  and  $W_t$  are the mass of specimens before and after soil burial, respectively.

## Attenuated Total Reflection-Fourier Transform Infrared Spectroscopy (ATR-FTIR)

ATR-FTIR of the parent polymer pairs and ENR/PBS simple blends was performed on Thermo Nicolet AVATAR 360 FTIR (Thermo Electron Corporation, Madison, USA). The infrared absorption spectra were recorded in the wavenumber ranges of 4000–400 cm<sup>-1</sup> with 4 cm<sup>-1</sup> resolution and 64 scans per sample.

## Results and Discussion

### Prediction of Phase Inversion and Co-continuous Phase

Phase inversion and co-continuous boundaries of the ENR/PBS simple blends could be effectively predicted based on the complex viscosity ( $\eta^*$ ) and apparent shear viscosity ( $\eta_s$ ) of the pure polymeric components. Figure 1 shows double-logarithmic plots of complex viscosity ( $\eta^*$ ) and apparent shear viscosity ( $\eta_s$ ) of pure PBS and ENR measured at 150 °C as a function of angular frequency and shear rate, respectively. It is clearly seen that the pure PBS showed lower complex viscosity and apparent shear viscosity than the pure ENR. This might be due to the higher molecular weight of ENR than PBS (i.e.,  $M_w$  of ENR = 390,000 g/mol [26] and PBS = 33,220 g/mol) [27]. Also, the chemical interaction between polar functional groups in epoxirane rings molecules might cause higher viscosity of ENR. Furthermore, the epoxirane rings in ENR molecular structures are easily cleaved under high temperature, moisture and shear force conditions which transform the rings to diol groups [28]. These diol groups are capable of interacting with other polar functional groups and also caused the self-crosslinking among the ENR molecular chains. Therefore, the molecular weight and molecular structure of ENR and PBS plays an important role in the flow resistance at temperatures either above the glass transition temperature of amorphous material or the melting temperature of semi-crystalline polymer (i.e., PBS) [8, 29].

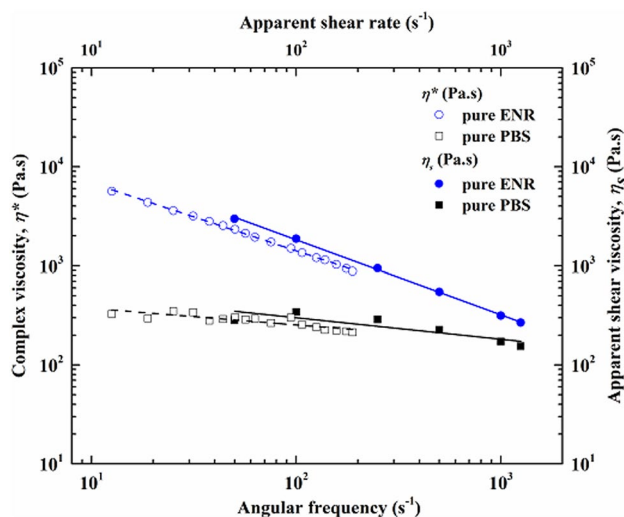


**Fig. 1** Shows double-logarithmic plots of complex viscosity ( $\eta^*$ ) (open symbols) and apparent shear viscosity ( $\eta_s$ ) (filled symbols) of pure PBS and ENR measured at 150 °C as a function of angular frequency and shear rate, respectively

In Fig. 1, the complex viscosity at various angular frequencies and the apparent shear viscosity at various apparent shear rates of the pure ENR and pure PBS can be approximated by the power law model of Ostwald–deWaele, as follow:

$$\eta^*(\omega) = K \times \omega^{n-1} \text{ or } \eta(\dot{\gamma}) = k \times \dot{\gamma}^{n-1} \quad (5)$$

where  $K$  and  $k$  are the consistency index and  $n$  is the power law index of the materials. In a double-logarithmic plot, the function defined in Eq. (5) turn into straight lines, where the slope of the straight line is equal to  $n-1$  and the value of  $K$  or  $k$  results from the intercept  $y_0$  on the y-axis. The straight lines plotted in Fig. 1 represent the results of least square fits of the corresponding experimental data. The obtained fit parameters, i.e., consistency index and power law index are summarized in Table 2.

An estimation of the shear rate in the internal mixer during the mixing process can be calculated by Eq. (6).

$$\text{Shear rate (s}^{-1}\text{)} = \frac{\pi \times d \times N}{h} \quad (6)$$

where  $N$  is the rotor speed (i.e., 60 rpm),  $d$  is the diameter of rotor (i.e., 72 mm) and  $h$  is the clearance (1.5 mm) of the internal mixer.

According to Eq. (6), the shear rate of the ENR/PBS blends during mixing operation at 120 °C and a rotor speed of 60 rpm is about  $150 \text{ s}^{-1}$ . Consequently, the complex viscosities and apparent shear viscosity of PBS ( $\eta_{PBS}$ ) and ENR ( $\eta_{ENR}$ ) were calculated according to Eq. (5) by inserting the corresponding fit parameters (Table 2) and the shear rate or angular frequency of  $150 \text{ s}^{-1}$ . It is noted, that according to Cox/Merz—relation the amount of the complex viscosity is equal to the shear viscosity at a certain shear rate, if the angular frequency of the complex viscosity is equal to the shear rate of the shear viscosity. The results are summarized in Table 2. It is seen that in both cases, complex viscosity (i.e., by RPA measurement) and shear flow properties (measured by high pressure capillary rheometer), the viscosity ratio is about 0.21.

In this work, the phase inversion and the co-continuous phase morphology of the ENR/PBS blends were predicted by several empirical and semi-empirical models [30]. Utracki et al. [21, 31, 32] predicted phase inversion of

**Table 2** Values of the parameters of the Ostwald–de Waele power law equation

Measurement Parameter	Complex viscosity		Shear flow properties	
	Pure PBS	Pure ENR	Pure PBS	Pure ENR
$K$ or $k$ (Pa s <sup>n</sup> )	549.6	33,066	814.1	59,421
$n$	0.8	0.3	0.8	0.2
$\eta$ @ $150 \text{ s}^{-1}$ (Pa s)	236.8	1071.4	274.3	1326.5

the polymer blends based on viscosity ratios of the blend components. Therefore, the Utracki model could be used to calculate the phase inversion behavior of ENR/PBS simple blend, as follows:

$$\phi_{ENR} = \frac{\left(1 - \log\left(\frac{\eta_{PBS}}{\eta_{ENR}}\right)\right) / [\eta]}{2} \tag{7}$$

where  $[\eta]$  is intrinsic viscosity, which was assumed as  $[\eta] = 1.9$  for spherical domains. The parameters  $\eta$  and  $\phi$  refer to the viscosity and volume fraction of the ENR and PBS components, respectively.

In addition, Paul and Barlow [22] calculated the phase inversion of the blends by extrapolating of the viscosity ratios, as follows:

$$\phi_{ENR} = \frac{1}{(1 + \eta_{PBS} / \eta_{ENR})} \tag{8}$$

Steinmann et al. [23] predicted the phase inversion approach based on the assumption that the shape relaxation times of the blend components reached the maximum state at the phase inversion composition. Therefore, strong correlation between the viscosity and elasticity ratios of the blend components was observed. Thus, the viscosity ratios at certain elasticity can be derived as follow:

$$\phi_{ENR} = -0.12 \log\left(\frac{\eta_{PBS}}{\eta_{ENR}}\right) + 0.48 \tag{9}$$

Furthermore, Gergen et al. [24] predicted the phase inversion based on the relationship between the viscosity ratios and the proportions of two components, as follow:

$$\log\left(\frac{\eta_{PBS}}{\eta_{ENR}}\right) = 2 - 4\phi_{ENR} \tag{10}$$

Figure 2 shows the phase inversion behavior based on relationship between volume fraction of ENR ( $\phi_{ENR}$ ) and viscosity ratios of blend components (i.e.,  $\eta_{PBS}/\eta_{ENR}$ ) that was predicted by Eqs. (7)–(10). It can be seen that the phase inversion occurs in the blend at the viscosity ratio (i.e.,  $\eta_{PBS}/\eta_{ENR}$ ) = 0.21, which is equivalent to the volume fractions of ENR = 0.67, 0.82, 0.56 and 0.66 (Table 3) according to the Utracki et al., Paul and Barlow, Steinmann et al., and Gergen et al., respectively. It can be seen that the weight fractions of ENR in the ENR/PBS blends for phase inversion at the volume fractions of 0.67, 0.82, 0.56 and 0.66 are approximately to 69, 84, 58 and 68 wt% (Table 3), respectively. This means that the co-continuous phase morphology of the blends by Steinmann model is agree with experimental data. This might be occurred at the blend ratio of ENR/PBS about 58/42 wt%.

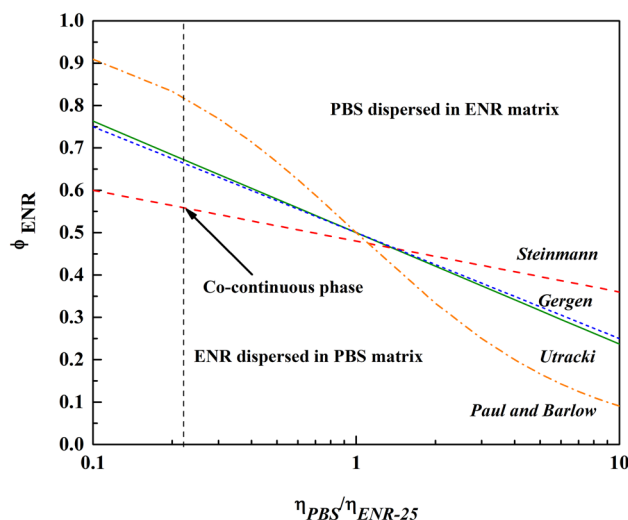


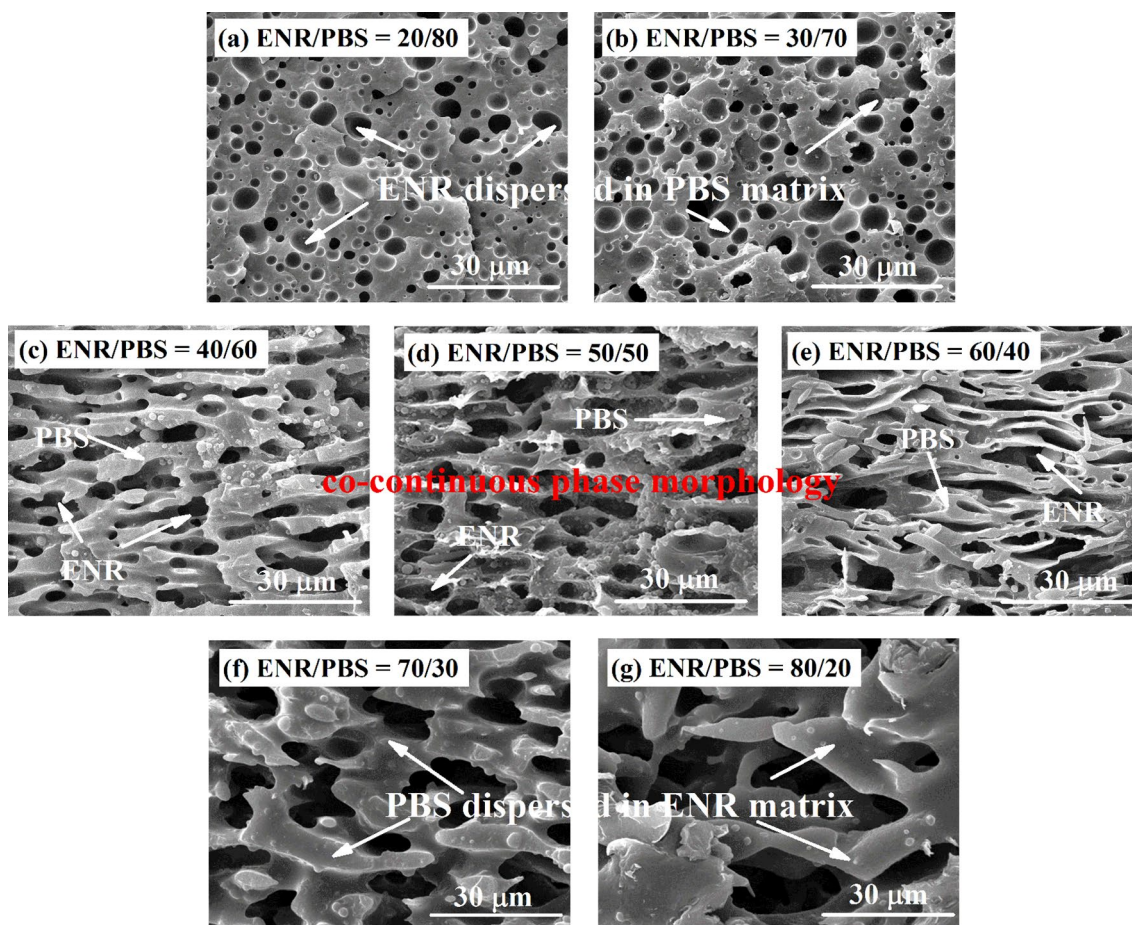
Fig. 2 Relationship between volume fraction of ENR ( $\phi_{ENR}$ ) and viscosity ratios of PBS and ENR predicted by four different models based on a constant shear rate of  $150 \text{ s}^{-1}$

Table 3 Volume and weight fractions of ENR in ENR/PBS blends at the first phase inversion predicted by different models

Models	Volume fraction of ENR ( $\phi_{ENR}$ )	Weight fraction of ENR (wt%)
Utracki et al.	0.68	70
Paul and Barlow	0.83	84
Steinmann et al.	0.56	58
Gergen et al.	0.67	69

### Morphological Properties

SEM micrographs of fractured surfaces of ENR/PBS simple blends with various blend ratios after extraction by toluene are shown in Fig. 3. It is clearly seen that all samples show the phase separated morphologies. That is, the small droplets of the ENR dispersed in the PBS matrix were observed in the ENR/PBS simple blend at 20/80 and 30/70 wt%, as seen in Fig. 3a, b. Furthermore, the co-continuous phase or dual phase morphologies were observed when the ENR/PBS = 40/60, 50/50 and 60/40 wt% (Fig. 3c–e). In addition, the finest co-continuous phase morphology was seen in the ENR/PBS blend ratio = 60/40 wt%. Therefore, the first phase inversion from dispersion of ENR droplets to the co-continuous phase morphology might be occurred at the blend ratio of ENR/PBS about 40/60 wt%. Then, the fully co-continuous phase with the fine grain morphology was developed in the ENR/PBS blend ratio of 60/40 wt%, which is very close to the predicted by the Steinmann et al. model at ENR/PBS blend ratios of 58/42 wt%.



**Fig. 3** SEM micrographs of ENR/PBS simple blends with various blend ratios: **a** 20/80, **b** 30/70, **c** 40/60, **d** 50/50, **e** 60/40, **f** 70/30 and **g** 80/20,  $\times 1500$

It is noted that the ENR/PBS blends with co-continuous phase structures may exhibit the TPE characteristics. In Fig. 3, it is seen that in the blends with ENR higher than 60 wt%, the transformation to the second phase inversion from the co-continuous phase morphology to the PBS droplets dispersed in the ENR matrix was observed, as seen in Fig. 3f, g. Therefore, it is concluded that the ENR/PBS simple blends showed the finest co-continuous phase morphologies at the ENR/PBS ratio around 60/40 wt% which correlated to the predicted results by the Steinmann et al. model in Fig. 2 and Table 3. Therefore, the Utracki et al., Paul and Barlow, and Gergen et al. models are not suitable to predict the composition of phase inversion of the ENR/PBS blends.

### Mechanical Properties

Stress–strain behaviors of pure PBS and ENR/PBS simple blends with various blend ratios are shown in Fig. 4. It is seen the pure PBS exhibits the highest slope at linear low strain region (i.e., Young’s modulus) of the stress–strain

curves. This is due to high stiffness of PBS which can be affirmed by the yield point of the stress–strain curve [17]. However, it is clearly seen that the yield point of PBS is drastically decreased when 20 wt% of the ENR was added and finally disappeared in the blends with ENR higher than 30 wt% where the materials become softer. It is also seen that Young’s modulus was decreased with increasing ENR contents due to lower stiffness of the materials.

Figure 5 shows mechanical properties in terms of tensile strength, elongation at break (Fig. 5a), 100% modulus, tension set (Fig. 5b), hardness (Shore A) and toughness (Fig. 5c) of ENR/PBS simple blends with various blend ratios. In Fig. 5a, it is seen the tensile strength decreased but elongation at break increased upon increasing of the ENR proportion. Furthermore, 100% modulus (Fig. 5b) also decreased with increasing of the ENR proportion, which correlates well to the Young’s modulus and stiffness of the blends (Fig. 4). In Fig. 5b, it is clear that the tension set decreased with increasing of the ENR proportion which reflects the enhancement of rubber elasticity. In addition, in Fig. 5c, hardness and toughness of the blends

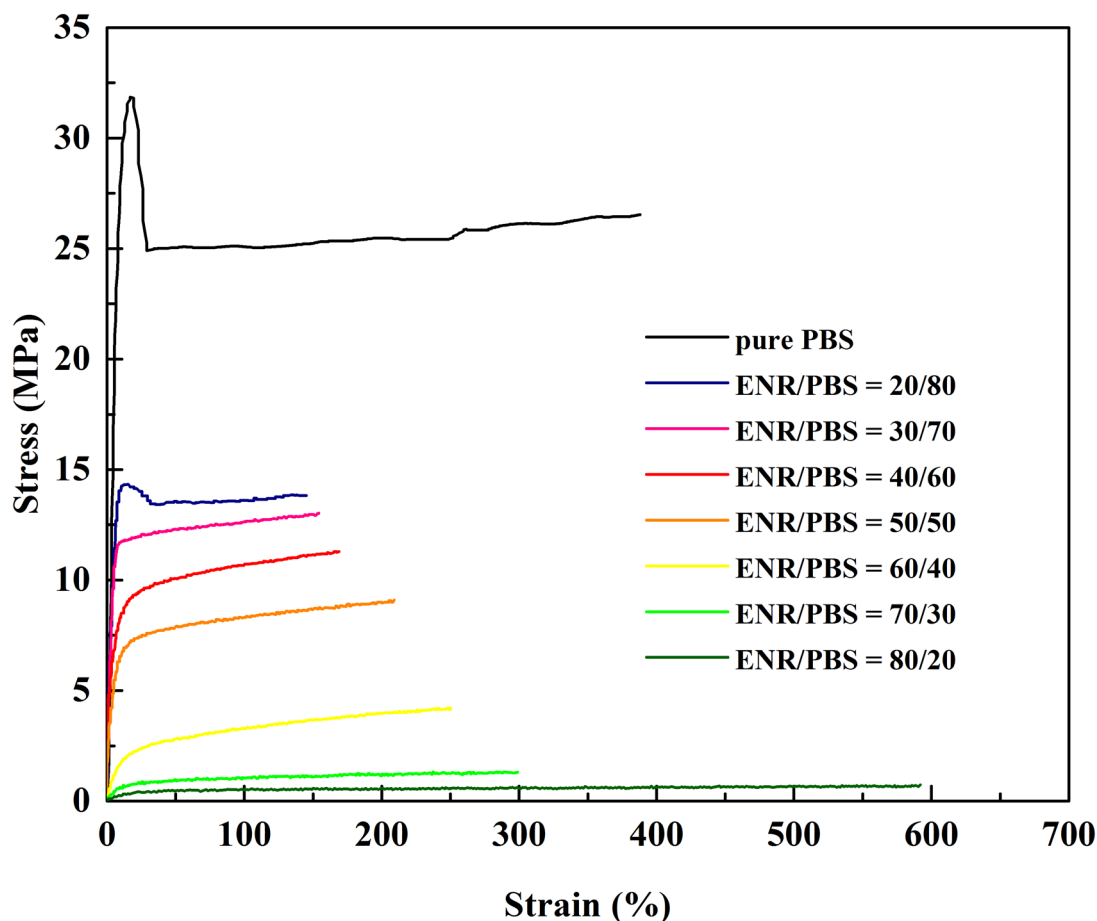


**Fig. 4** Stress–strain curves of pure PBS and ENR/PBS simple blends with various blend ratios

also decreased with increasing of the ENR proportions. It is noticed that strong decrease of these properties was observed in the blends with ENR proportions about 50 wt% and above where the first phase inversion occurred. Therefore it is concluded that the optimum rubberlike properties of the blends were achieved at the ENR/PBS ratio about 60/40 wt% which is well correlated to the predicted model of Steinmann (Fig. 2) and morphological properties (Fig. 3). In addition, it is clearly seen in Fig. 5a–c that the mechanical properties of the blends were abruptly changed again when the ENR proportions were greater than 70 wt% where the second phase inversion took place. Here, the co-continuous phase was gradually modified to the PBS droplets dispersed in the ENR matrix.

### Thermal Properties

Thermal properties of the ENR/PBS blends were investigated by differential scanning calorimetry (DSC). Figure 6 shows DSC thermograms of the pure parent polymer pairs (i.e., ENR and PBS) and ENR/PBS blends with different blend ratios. Also, Table 4 summarizes crystallization

temperature ( $T_c$ ), glass transition temperature ( $T_g$ ), melting temperature ( $T_m$ ) and degree of crystallinity ( $X_c$ ) of pure parent polymer pairs and ENR/PBS blends that were evaluated based on DSC thermograms in Fig. 6. It is noted that the degree of crystallinity of PBS in ENR/PBS blends could be evaluated by Eq. (7) [9].

$$\text{Degree of crystalline } (\%X_c) = \frac{\Delta H_m}{\Delta H_m^0} \times \frac{100}{W} \quad (11)$$

where  $\Delta H_m$  is the melting enthalpy,  $\Delta H_m^0$  is the melting enthalpy for 100% crystalline PBS which is 110.3 J/g [9], and  $W$  is the weight fraction (wt%) of PBS in the ENR/PBS blends.

In Fig. 6 and Table 4, it is seen that the  $T_g$  of pure ENR with 50 mol% is about  $-21.3$  °C, while the  $T_g$ ,  $T_c$  and  $T_m$  of the pure PBS are  $-29.6$ ,  $81.3$  and  $116.0$  °C, respectively. It is also seen that the degree of crystallinity ( $X_c$ ) of pure PBS is about 51.7% (Table 4). However, the  $X_c$  of PBS in the blends was increased with increasing ENR proportions in the ranges 20–30 wt% to gain the maximum  $X_c$  of 60.5% at ENR proportion of 30 wt%. This might be due

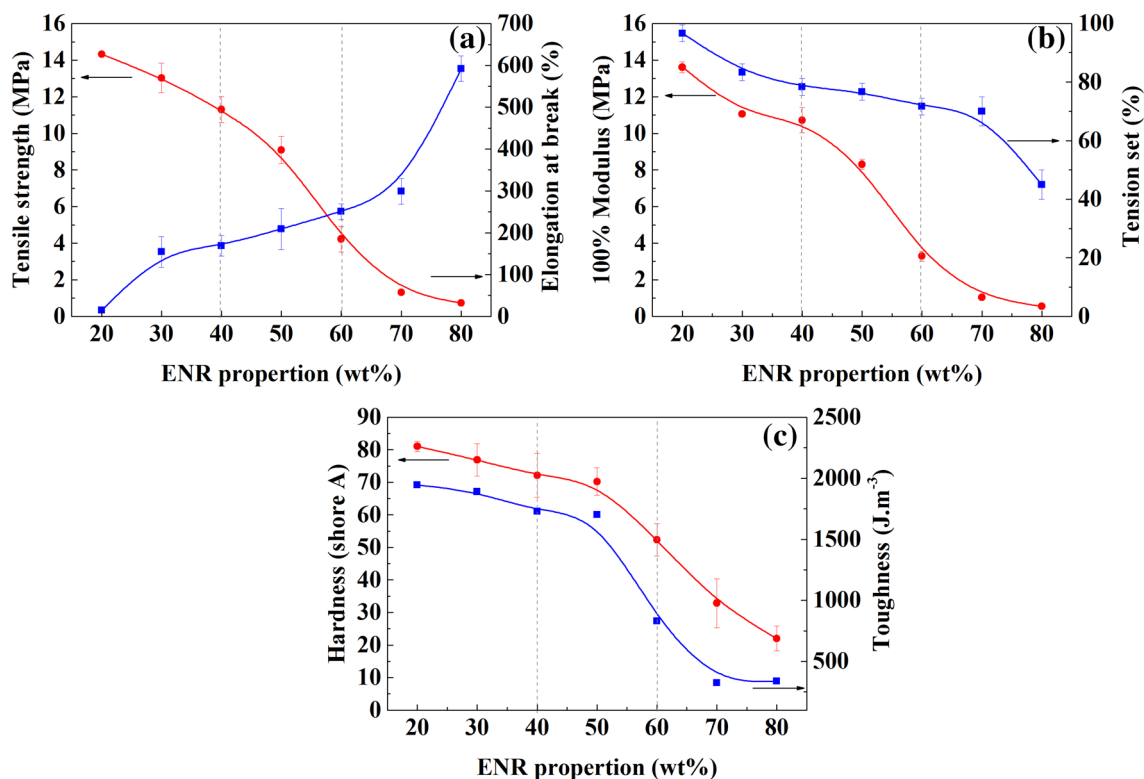


**Fig. 5** Tensile strength and elongation at break (a), 100% modulus and tension set (b) and hardness and toughness properties (c) of ENR/PBS simple blends with various ENR proportions

to the ENR droplets act as the nucleating agent for the crystalline growth of the PBS molecules. Upon increasing ENR proportions to 40 wt% and above, decreasing trend of the  $X_c$  was observed. This might be due to morphological evolution from dispersion of ENR droplets in PBS to co-continuous or dual phase morphology at the first inversion boundary at about ENR/PBS = 40/60. In addition, in the second phase inversion from co-continuous structure to dispersion of PBS droplets in ENR matrix occurred in the blends with ENR higher than 60 wt% (i.e., 70/30 and 80/20 wt%), decreasing trend of  $X_c$  was also found until the lowest value at 35.3%. This might be due to ENR is a major phase or matrix that could not enter into the PBS phase to start the nucleation. In a conclusion, it is obvious that the trend of  $X_c$  is correlated well to the evolution of morphological properties (Fig. 3) and mechanical properties (Figs. 4, 5). That is, in the blends with 20–30 wt% of ENR, the ENR phase behaves as small droplets which dispersed in PBS matrix. Hence, the ENR droplets could nucleate and propagate the crystalline growth of the PBS phase in ENR/PBS simple blends. These droplets also causes increasing of the interfacial adhesion among ENR and PBS molecules and therefore caused more crystalline growth in PBS and hence increasing of the  $X_c$  [9, 33].

## Biodegradability

Biodegradability of the ENR/PBS simple blends with various blend ratios was investigated by the digital microscope and SEM micrographs after soil burial for 9 months, as results seen in Figs. 7 and 8, respectively. It is clear that the buried samples showed rough surfaces owing to the biodegradability caused by the activity of microorganism, as small holes observed in pure PBS [34] in Fig. 7a. However, these holes are more distinguished after addition of ENR and it is seemingly to be increased with increasing ENR proportion from 20 to 80 wt%, as presented in Fig. 7b–h, respectively. This clarifies that the ENR is biopolymer with some non-rubber contents like protein and lipids [35] which encourages the biodegradation of the ENR/PBS blends relative to the pure PBS. It is noted that the degradation degree might be related to the oxidative attractions at the double bonds of ENR molecular chains [36]. Thus, addition of ENR might favor the biodegradability of the ENR/PBS blends since the ENR molecular chains are also capable of naturally degrading, particularly when the first phase inversion is occurred at ENR proportion at 40–60 wt%, as seen in Fig. 7d–f. In addition, strong biodegradability of the ENR/PBS blends was clearly observed after the second phase inversion in the



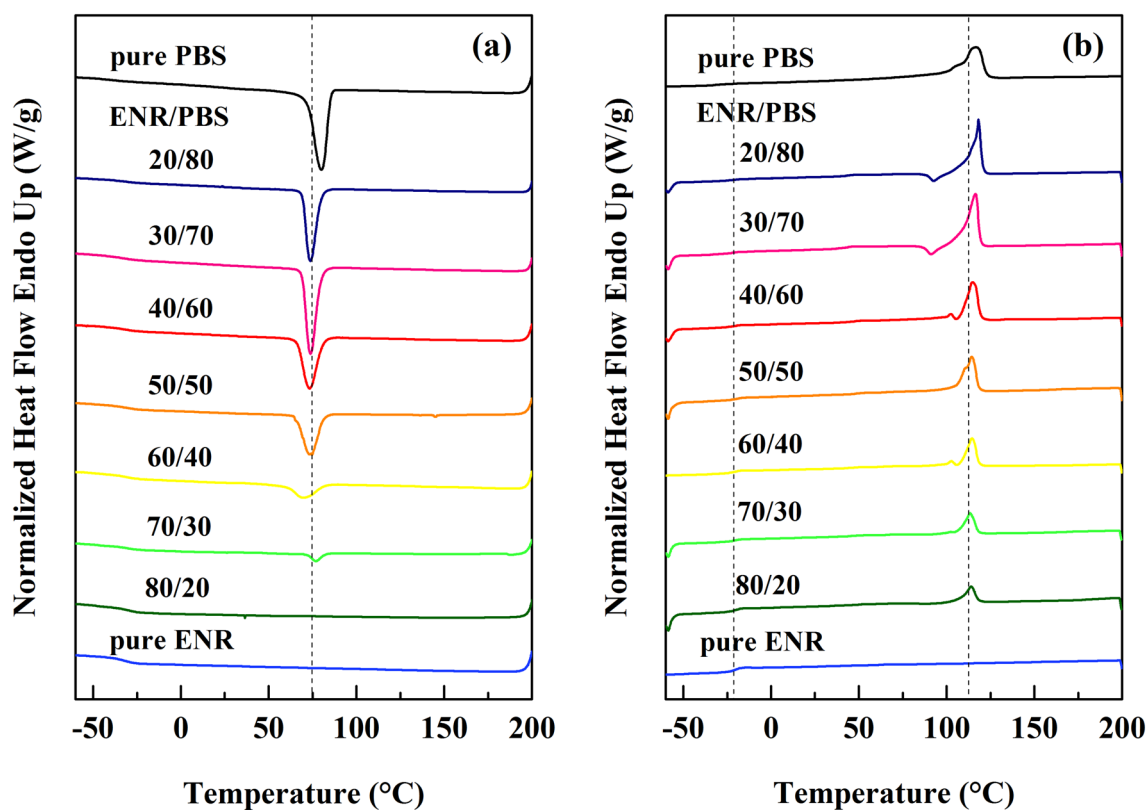


**Fig. 6** DSC thermograms of pure ENR, pure PBS and ENR/PBS simple blends; cooling scan (200 to  $-60$  °C) (a) and 2nd heating scan ( $-60$  to 200 °C) (b)

**Table 4** Thermal properties in terms of crystallization ( $T_c$ ), glass transition ( $T_g$ ), crystalline melting temperatures ( $T_m$ ) and degree of crystallization ( $X_c$ ) of pure ENR and PBS together with ENR/PBS blends with various blend ratios

ENR proportion (wt%)	$T_c$ (°C)	$T_g$ (°C)	$T_m$ (°C)	$X_c$ (%)
Pure PBS	81.3	-29.6	116.0	51.7
20	74.7	-21.6	113.8	45.9
30	80.1	-20.4	113.7	60.5
40	74.0	-20.8	113.8	53.1
50	75.2	-21.6	113.5	52.8
60	69.6	-20.1	113.9	50.7
70	76.8	-19.9	113.4	45.9
80	-	-20.5	113.5	35.3
Pure ENR	-	-21.3	-	-

blends with ENR proportions of 70 and 80 wt%, respectively, as seen in Fig. 7g, h. Here, the microorganism could be detected by the digital microscope, as seen as the white dots in the buried samples. These gram positive characteristics of microorganism might be utilized to the molecular chains of the blends as a sole source of energy generating an enzyme that further hydrolyze glucosidic linkages in the

degradable mechanism in the ENR/PBS blends, particularly in the ENR phase [37]. However, higher biodegradability of ENR/PBS blends was found in the blends with ENR proportions of 70–80% might be due to lower degree of crystallinity ( $X_c$ ), especially in the blend with 80 wt% of ENR which had the  $X_c$  lower than the  $X_c$  of pure PBS [38]. Hence, the loose structure of ENR/PBS blends might promote the ease of microorganism movement into the blends in particular in the PBS phase with low crystalline content. In addition, the micrographs from the digital micrographs are well agreement with the SEM images with higher magnification. That is, the smooth surface with small holds of pure PBS was observed (Fig. 8a). Also, the soil buried samples surfaces were rougher when the ENR was added. Furthermore, the microorganism spots were also detected by the SEM images which can be clearly distinguished after ENR proportion over 20 wt% (i.e., Fig. 8b–h).

Figure 9 shows weight loss of the pure PBS and ENR/PBS simple blends with various blend ratios after the soil burial tests of 1, 3 and 9 months. It is clearly seen that significant difference weight loss which indicates degree of degradation of pure PBS and ENR/PBS simple blends with different blend proportions and soil burial periods was observed. That is, the weight loss of the pure PBS and ENR/

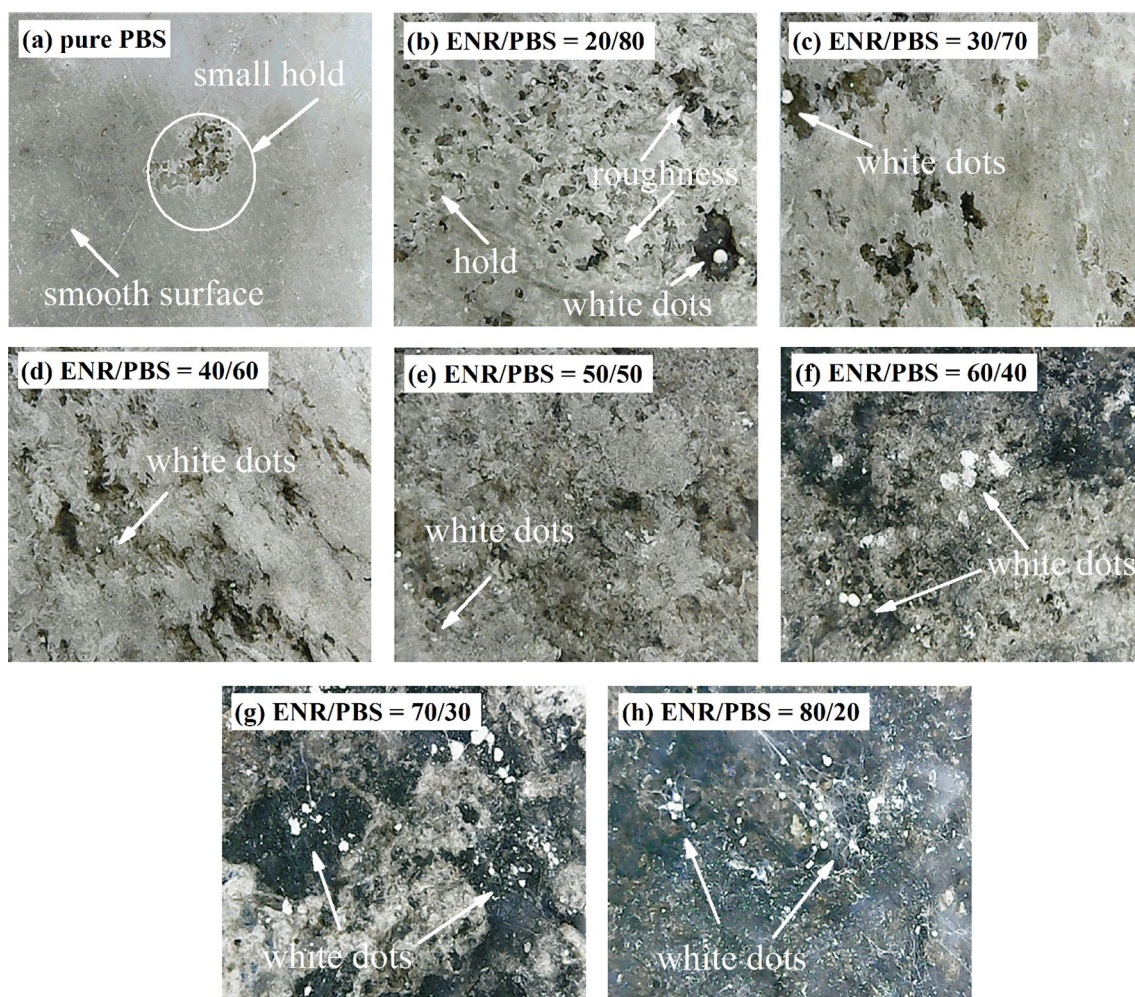


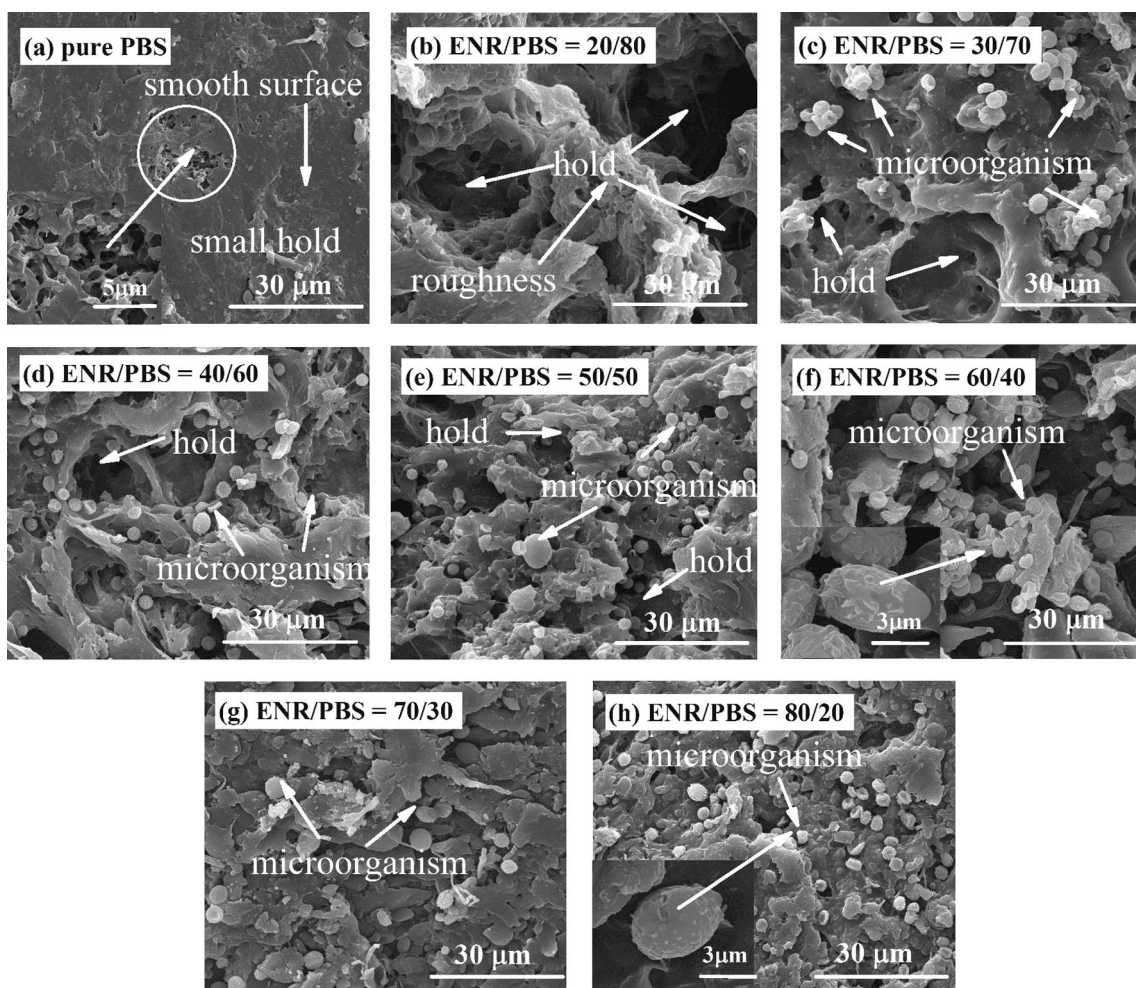
**Fig. 7** Digital microscope micrographs of ENR/PBS simple blends with various blend ratios: pure PBS (a), 20/80 (b), 30/70 (c), 40/60 (d), 50/50 (e), 60/40 (f), 70/30 (g) and 80/20 (h) after soil burial test for 9 months

PBS blends showed no significant difference for the burial duration of 1 month. However, the weight loss were slightly increased after 3 months soil burial test. That is, the weight loss showed linearly increased with increasing of the ENR proportions. The degradation by decreasing of weight loss was clearly distinguished after 9 months burial test. That is, non-linear degradation rate was found after addition of ENR phase. Furthermore, the blends with ENR about 20–50 wt% after soil burial for 9 months showed no significant differences in the weight losses until the second phase inversion from the co-continuous phase of ENR and PBS to dispersion of PBS droplets in ENR matrix occurred at the ENR content about 60 wt%. Above this ENR proportion, the weight loss of ENR/PBS simple blends showed abruptly increased. This might be due to the second phase inversion of the blends that transform from the co-continuous structure to PBS droplets dispersed in ENR matrix. Thus, the microorganism can easily enter and degrade the ENR matrix which covers the PBS droplets in the blends and finally higher degradation rate was

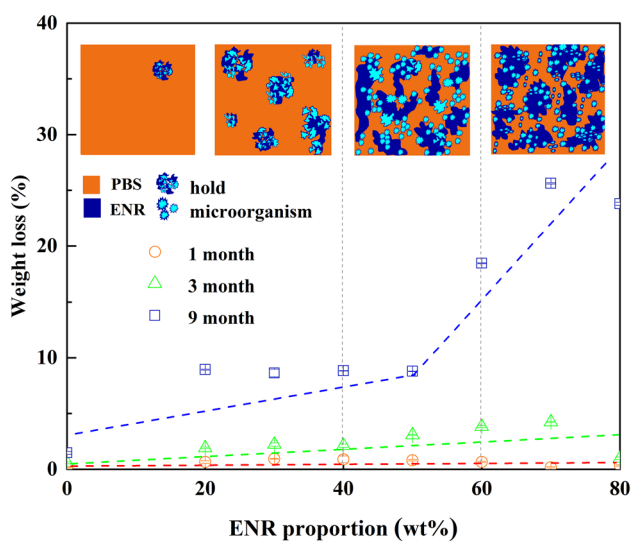
found. This well correlates to the digital and SEM micrographs (Figs. 8, 9, respectively) where clearly indicated the first and second phase inversions in the blends with different blend proportions.

### ATR-FTIR Analysis

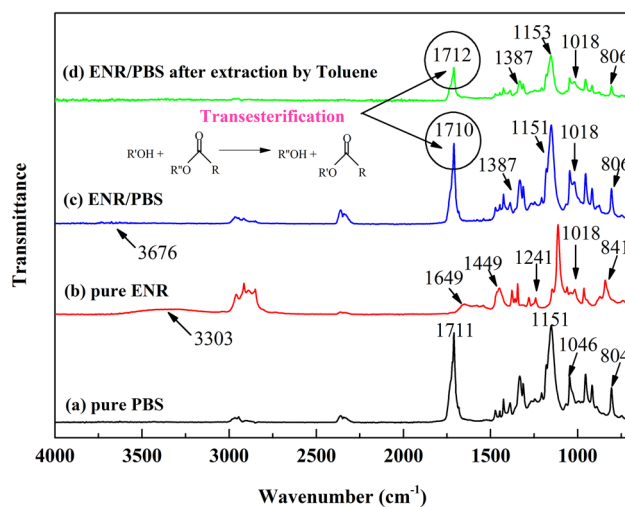
Infrared spectroscopy was exploited to characterize the structural changes and the interaction between ENR and PBS molecules in the ENR/PBS blends. Figure 10 shows ATR-FTIR spectra of pure parent polymer pairs (i.e., ENR and PBS) and ENR/PBS blends with and without toluene extraction. Also, the corresponded potential FTIR peaks in Fig. 10 are summarized in Table 5. It can be seen that the pure PBS (Fig. 10a) showed the characteristic absorption peaks at the wavenumbers of 804, 1046, 1151 and 1711  $\text{cm}^{-1}$  which assign to C–H out of plane bending, O–C–C stretching, C–C stretching and C=O stretching vibrations of the PBS molecules, respectively [39]. In Fig. 10b, the absorption



**Fig. 8** SEM micrographs of ENR/PBS blends with various blend ratios pure PBS (a), 20/80 (b), 30/70 (c), 40/60 (d), 50/50 (e), 60/40 (f), 70/30 (g) and 80/20 (h) after soil burial test for 9 months



**Fig. 9** Weight loss of the pure PBS and ENR/PBS simple blends with various blend ratios after the soil burial tests of 1, 3 and 9 months

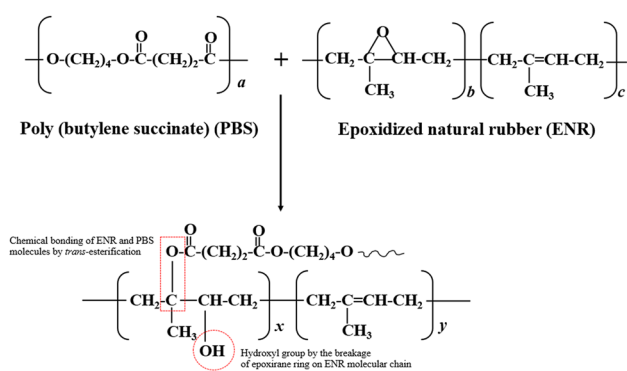


**Fig. 10** ATR-FTIR spectra of pure PBS (a), pure ENR (b), ENR/PBS blends (c), ENR/PBS blends after extraction by toluene (d)

**Table 5** Peak assignments of the infrared spectra showed in Fig. 10

Wavenumber (cm)	Assignments
	Pure PBS
804	C–H (out of plane bending vibration)
1046	O–C–C stretching vibration
1151	C–C stretching vibration
1711	C=O stretching vibration
	Pure ENR
841	=C–H (out of plane bending vibration)
871	C–O stretching vibration
1018	O–C stretching vibration
1241	C–O–C stretching vibration
1449	C–H stretching vibration
1649	C=C (double bonds) stretching vibration
3303	O–H groups stretching vibration (i.e., hydroxyl or glycol)
	ENR/PBS blend
806	CH (out of plane bending vibration)
1018	O–C stretching vibration
1151	C–C stretching vibration
1387	C–O–C stretching vibration
1710	C=O stretching vibration
3676	O–H stretching vibration

peaks at the wavenumbers of 841, 871, 1018, 1241, 1449, 1649 and 3303  $\text{cm}^{-1}$  which correspond to the C–H double bond (=C–H) out of plane bending, asymmetric epoxide ring (O–C) stretching, asymmetric O–C stretching in alcohol, symmetric C–O–C stretching, asymmetric C–H stretching, double bonds (C=C) stretching and broad absorption of hydroxyl groups (e.g. hydroxyl and glycol) stretching vibrations [39–43], respectively, in ENR molecules were observed. In addition, the FTIR spectrum of ENR/PBS blends (Fig. 10c), the absorption peaks at 806, 1018, 1151 and 1710  $\text{cm}^{-1}$  were found. They refer to C–H out of plane bending, O–C stretching, C–C stretching and C=O stretching vibrations of PBS molecules. Furthermore, the peaks at 1387 and at 3676  $\text{cm}^{-1}$  which referred to C–O–C stretching and OH stretching vibrations of ENR molecules were also found. In addition, the absorption peak at 1710  $\text{cm}^{-1}$ , which is assigned to C=O stretching vibrations due to chemical reaction between functional groups in ENR and PBS molecules through the trans-esterification reaction during blending operation was observed, as described in Scheme 1. It is noted that the epoxide groups in ENR molecules are easily to be broken by heat and moisture before giving the diol functional groups. These groups are capable of continuously interacting with polar ester groups in PBS molecules by esterification and might be further caused ENR–PBS chemical linkages. This chemical interaction between ENR

**Scheme 1** A proposed reaction between ENR and PBS molecules

and PBS molecules is confirmed by the appearance of the absorption peaks at 1710  $\text{cm}^{-1}$  of C=O stretching vibrations [44]. In Fig. 10d, the ENR/PBS blend with toluene extraction to completely remove the ENR phase existed in the blends. It is clearly seen that the absorption peaks which indicates chemical interactions at 1710  $\text{cm}^{-1}$  of the C=O stretching vibrations is still existed. This confirms existence of the chemical reaction between ENR and PBS phases. Therefore, it is concluded that the chemical interaction between ENR and PBS molecules in the ENR/PBS simple blends can possibly occur during processing and influences on mechanical and other related properties of the blends (Fig. 5).

## Conclusion

The co-continuous phase and phase inversion of ENR/PBS blends were investigated. The empirical and semi-empirical models were used to predict the evolution of phase inversion of the blends. It was found that the Steinmann model showed the phase inversion of ENR/PBS blend at the volume fraction of ENR ( $\phi_{ENR}$ ) at 0.56%v which is equivalent to weight fraction of 58 wt%. Therefore, the first co-continuous structure was predicted by the Steinmann model at the ENR/PBS = 58/42 wt%. This is in good agreement with morphological properties and other related properties. That is, the morphological properties of the blends with various blend ratios indicated the co-continuous phase morphologies in the ENR/PBS = 40/60, 50/50 and 60/40 wt%. Therefore, increasing ENR contents higher than 60 wt% caused the second phase inversion where the co-continuous phase was transformed to dispersion of PBT droplets in the ENR matrix. In addition, degree of crystallinity of PBS in the ENR/PBS blends increased with increasing ENR proportion below the first phase inversion (i.e., ENR = 20–30 wt%). However, the degree of crystallinity of PBS showed decreasing trend when the ENR proportion > 60 wt% where the second phase

inversion occurred. This relates to the biodegradability of the ENR/PBS blends which was strongly degraded in the blends with ENR proportion over 60 wt% where the ENR is a matrix. Therefore, it is concluded that the co-continuous phase structure of the blends occurred at ENR contents in the ranges 40–60 wt%. In a conclusion, novel biodegradable TPEs based on PBS and ENR blends with optimum mechanical properties and biodegradability was successfully prepared.

**Acknowledgements** This research was financially supported by a grant from the Higher Education Research Promotion and National Research University Project of Thailand, Office of the Higher Education Commission, contract No. SIT580647S, by the Thailand Research Fund (TRF) through the Royal Golden Jubilee Ph.D. Program (Grant No. PHD/0208/2557) to Dr. Charoen Nakason as principal researcher, and to Miss Parisa Faibunchan as the research assistant and by Prince of Songkla University, Surat Thani Campus. The authors would like to express their gratitude to the University of Applied Science, Osnabrück, Germany, for their research facilities and the other supports.

## References

- Samia B, Farid R (2014) Dynamic mechanical and thermal properties of a chemically modified polypropylene/natural rubber thermoplastic elastomer blend. *Polym Test* 36:54–61
- Nakason C, Wannavilai P, Kaesaman A (2006) Effect of vulcanization system on properties of thermoplastic vulcanizates based on epoxidized natural rubber/polypropylene blends. *Polym Test* 25:34–41
- Nakason C, Jarnthong M, Kaesaman A, Kiatkamjornwong S (2009) Influences of blend proportions and curing systems on dynamic, mechanical, and morphological properties of dynamically cured epoxidized natural rubber/high-density polyethylene blends. *Polym Eng Sci* 49:281–292
- Mousa A, Ishiaku US, Mohd Ishak ZA (2000) Rheological properties of dynamically vulcanized poly(vinyl chloride)/epoxidized natural rubber thermoplastic elastomers: effect of processing variables. *Polym Test* 19:193–204
- Ishiaku US, Shaharum A, Ismail H, Mohd Ishak ZA (1998) The effect of an epoxidized plasticizer on the thermo-oxidative ageing of poly(vinyl chloride)/epoxidized natural rubber thermoplastic elastomers. *Polym Int* 45:83–91
- Nakason C, Narathichat M, Kummerlöwe C, Vennemann N (2012) Thermoplastic natural rubber based on polyamide-12 blended with various types of natural rubber: effect of processing oils and plasticizer. *J Elastomers Plast* 45:47–75
- Romin R, Nakason C, Thitithammawong A (2013) Thermoplastic elastomer based on epoxidized natural rubber/polyamide-12 and co-polyamide-12 blends. *Adv Mater Res* 626:58–61
- Mishra J, Chang YW, Kim DK (2007) Green thermoplastic elastomer based on polycaprolactone/epoxidized natural rubber blend as a heat shrinkable material. *Mater Lett* 61:3551–3554
- Wahit MU, Hassan A, Ibrahim AN, Zawawi NA, Kunasegeran K (2015) Mechanical, thermal and chemical resistance of epoxidized natural rubber toughened polylactic acid blends. *Sains Malays* 44:1615–1623
- Mendes JF, Paschoalin RT, Carmona VB, Neto ARS, Marques ACP, Marconcini JM, Mattoso LHC, Medeiros ES, Oliveira JE (2016) Biodegradable polymer blends based on corn starch and thermoplastic chitosan processed by extrusion. *Carbohydr Polym* 137:452–458
- Liu D, Qi Z, Zhang Y, Xu J, Guo B (2015) Poly(butylene succinate) (PBS)/ionic liquid plasticized starch blends: preparation, characterization, and properties. *Starch-Stärke* 67:802–809
- Bhatia A, Gupta Rahul K, Bhattacharya Sati N, Choi HJ (2007) Compatibility of biodegradable poly (lactic acid) (PLA) and poly (butylene succinate) (PBS) blends for packaging application. *Korea-Aust Rheol J* 19:125–131
- Hassan E, Wei Y, Jiao H, Muhuo Y (2013) Dynamic mechanical properties and thermal stability of poly(lactic acid) and poly(butylene succinate) blends composites. *J Fiber Bioeng Inform* 6:85–94
- Stoyanova N, Paneva D, Mincheva R, Toncheva A, Manolova N, Dubois P, Rashkov I (2014) Poly(L-lactide) and poly(butylene succinate) immiscible blends: from electrospinning to biologically active materials. *Mater Sci Eng C* 41:119–126
- Wang R, Wang S, Zhang Y, Wan C, Ma P (2009) Toughening modification of PLLA/PBS blends via in situ compatibilization. *Polym Eng Sci* 49:26–33
- Yin Q, Chen F, Zhang H, Liu C (2015) Mechanical properties and thermal behavior of TPS/PBS blends with maleated PBS as a compatibilizer. *Adv Mater Res* 1119:306–309
- Hemsri S, Thongpin C, Moradokpermpoon N, Niramom P, Suppaso M (2015) Mechanical properties and thermal stability of poly(butylene succinate)/acrylonitrile butadiene rubber blend. *Macromol Symp* 354:145–154
- Jamaluddin N, Razaina MT, Mohd Ishak ZA (2016) Mechanical and morphology behaviours of polybutylene (succinate)/thermoplastic polyurethane blend. *Proc Chem* 19:426–432
- Pichaiyut S, Wisunthorn S, Thongpet C, Nakason C (2016) Novel ternary blends of natural rubber/linear low-density polyethylene/thermoplastic starch: influence of epoxide level of epoxidized natural rubber on blend properties. *Iran Polym J* 25:711–723
- Tanrattanakul V, Bunkaew P (2014) Effect of different plasticizers on the properties of bio-based thermoplastic elastomer containing poly(lactic acid) and natural rubber. *Express Polym Lett* 8:387–396
- Utracki LA (1991) On the viscosity-concentration dependence of immiscible polymer blends. *J Rheol* 35:1615–1637
- Paul DR, Barlow JW (1980) Polymer blends (or Alloys). *J Macromol Sci Rev Macromol Chem Phys* 18:109–168
- Steinmann S, Gronski W, Friedrich C (2001) Cocontinuous polymer blends: influence of viscosity and elasticity ratios of the constituent polymer on phase inversion. *Polymer* 42:6619–6629
- Gergen WP, Lutz RG, Davison S (1996) Hydrogenated block copolymers in thermoplastic elastomer interpenetrating polymer networks. In: Holden G, Legge NR, Quirk R, Schroeder HE (eds) *Thermoplastic elastomers*, 2nd edn. Hanser Publisher, Munich
- Mitsuyoshi F, Youtoku K (1991) Rheological properties of polypropylene/ high-density polyethylene blend melts. I. capillary flow properties. *J Appl Polym Sci* 42:467–480
- Poh BT, Yong AT (2009) Dependence of peel adhesion on molecular weight of epoxidized natural rubber. *J Adhes* 85:435–446
- Yoo E, Im SS (1999) Melting behavior of poly(butylene succinate) during heating scan by DSC. *J Polym Sci Part B: Polym Phys* 37:1357–1366
- Gelling IR (1991) Epoxide natural rubber. *J Nat Rubber Res* 6:184–205
- Nakason C, Jamjinno S, Kaesaman A, Kiatkamjornwong S (2008) Thermoplastic elastomer based on high-density polyethylene/natural rubber blends: rheological, thermal, and morphological properties. *Polym Adv Technol* 19:85–98
- Favis BD, Chalifoux JP (1988) Influence of composition on the morphology of polypropylene/polycarbonate blends. *Polymer* 29:1761–1767

31. Mekhilef N, Verhoogt H (1996) Phase inversion and dual-phase continuity in polymer blends: theoretical predictions and experimental results. *Polymer* 37:4069–4077
32. Han MS, Seo WJ, Paik HS, Hyun JC, Lee JW, Kim WN (2003) Rheological properties and phase inversion of polypropylene and poly(styrene-co-acrylonitrile) blends. *Polym J* 35:127–132
33. Pongtanayut K, Thongpin C, Santawitee O (2013) The effect of rubber on morphology, thermal properties and mechanical properties of PLA/NR and PLA/ENR blends. *Energy Procedia* 34:888–897
34. Anankaphong H, Pentrakoon D, Junkasem J (2015) Effect of rubberwood content on biodegradability of poly(butylene succinate) biocomposites. *Int J Polym Sci* 1–9
35. Eng AH, Tanaka Y, Gan SN (1997) Some properties of epoxidised deproteinised natural rubber. *J Nat Rubber Res* 12:82–89
36. Fainleib A, Renata VP, Elizabete FL, Bluma GS (2013) Degradation of non-vulcanized natural rubber-renewable resource for fine chemicals used in polymer synthesis. Institute of Macromolecular Chemistry, The National Academy of Sciences of Ukraine, NASU, Kyiv
37. Afiq MM, Azura A (2013) Effect of sago starch loadings on soil decomposition of natural rubber latex (NRL) composite films mechanical properties. *Int Biodeterior Biodegradation* 85:139–149
38. Tserki V, Matzinos P, Pavlidou E, Vachliotis D, Panayiotou C (2006) Biodegradable aliphatic polyesters. Part I. properties and biodegradation of poly(butylene succinate-co-butylene adipate). *Polym Degrad Stab* 91:367–376
39. Llorens E, Ibañez H, Valle LJ del, Puiggali J (2015) Biocompatibility and drug release behavior of scaffolds prepared by coaxial electrospinning of poly(butylene succinate) and polyethylene glycol. *Mater Sci Eng* 49:472–484
40. Wichian AN (2013) Preparation and mechanical property of the epoxidized natural rubber from field latex. *Rubber Thai J* 2:1–8
41. Salaeh S, Nakason C (2012) Influence of modified natural rubber and structure of carbon black on properties of natural rubber compounds. *Polym Compos* 33:489–500
42. Nakaramontri Y, Nakason C, Kummerlowe C, Vennemann N (2015) Effects of in-situ functionalization of carbon nanotubes with bis(triethoxysilylpropyl) tetrasulfide (TESPT) and 3-aminopropyltriethoxysilane (APTES) on properties of epoxidized natural rubber-carbon nanotube composites. *Polym Eng Sci* 55:2500–2510
43. Nakaramontri Y, Nakason C, Kummerlowe C, Vennemann N (2016) Enhancement of electrical conductivity and filler dispersion of carbon nanotube filled natural rubber composites by latex mixing and in situ silanization. *Rubber Chem Technol* 89:272–291
44. Gong-Peng L, Ling L, Xiu-Li W, Li C, Yu-Zhong W (2015) PBT/PC blends compatibilized and toughened via copolymers in situ formed by mgo-catalyzed transesterification. *Ind Eng Chem Res* 54:1282–1291